

# In vivo evaluation of a novel $^{18}\text{F}$ -labeled PET radioligand for translocator protein 18kDa (TSPO) in monkey brain

Xuefeng Yan (✉ [xuefeng.yan@nih.gov](mailto:xuefeng.yan@nih.gov))

National Institute of Mental Health <https://orcid.org/0000-0002-9803-5222>

**Fabrice G. Siméon**

National Institutes of Health

**Jeih-San Liow**

National Institutes of Health

**Cheryl L. Morse**

National Institutes of Health

**Jose A. Montero Santamaria**

National Institutes of Health

**Madeline Jenkins**

National Institutes of Health

**Lester S. Manly**

National Institutes of Health

**Maia Van Buskirk**

National Institutes of Health

**Sami S. Zoghbi**

National Institutes of Health

**Victor W. Pike**

National Institutes of Health

**Robert B. Innis**

National Institutes of Health

**Paolo Zanotti-Fregonara**

National Institutes of Health

---

## Research Article

**Keywords:**  $^{18}\text{F}$ -SF51, TSPO, PET, brain, monkey

**Posted Date:** October 24th, 2022

**DOI:** <https://doi.org/10.21203/rs.3.rs-2167175/v1>

**License:**  This work is licensed under a Creative Commons Attribution 4.0 International License.

[Read Full License](#)

---

**Version of Record:** A version of this preprint was published at European Journal of Nuclear Medicine and Molecular Imaging on May 30th, 2023. See the published version at <https://doi.org/10.1007/s00259-023-06270-9>.

# Abstract

**Purpose:**  $^{18}\text{F}$ -SF51 was previously found to have high binding affinity and selectivity for 18kDa translocator protein (TSPO) in mouse brain. This study sought to further evaluate the suitability of  $^{18}\text{F}$ -SF51 for absolute quantification of TSPO in monkey brain.

**Methods:** Positron emission tomography (PET) imaging was performed in monkey brain ( $n=3$ ) at baseline and after pre-blockade with the TSPO ligands PK11195 and PBR28. TSPO binding was calculated as total distribution volume corrected for free parent fraction in plasma ( $V_T/f_p$ ) using a two-tissue compartment model. Receptor occupancy and nondisplaceable uptake were determined via Lassen plot. Binding potential ( $BP_{ND}$ ) was calculated as the ratio of specific binding to nondisplaceable uptake. Time stability of  $V_T$  was used as an indirect probe to detect radiometabolite accumulation in the brain. *In vivo* and *ex vivo* experiments were performed in mice to determine the distribution of the radioligand.

**Results:** After  $^{18}\text{F}$ -SF51 injection, the concentration of brain radioactivity peaked at 2.0 standardized uptake value (SUV) at  $\sim 10$  minutes and declined to 30% of the peak at 180 minutes.  $V_T/f_p$  at baseline was generally high ( $203 \pm 15 \text{ mL} \cdot \text{cm}^{-3}$ ) and decreased by  $\sim 90\%$  after blockade with PK11195.  $BP_{ND}$  of the whole brain was  $7.6 \pm 4.3$ .  $V_T$  values reached levels similar to terminal 180-minute values by 70 minutes and remained relatively stable thereafter with excellent identifiability (standard errors  $< 5\%$ ), suggesting that no significant radiometabolites accumulated in the brain. *Ex vivo* experiments in mouse brain showed that 96% of radioactivity was parent. No significant uptake was observed in the skull, suggesting a lack of defluorination *in vivo*.

**Conclusion:** The results demonstrate that  $^{18}\text{F}$ -SF51 is an excellent radioligand with a good ratio of specific to nondisplaceable uptake as well as good time stability of total receptor binding. Collectively, the results suggest that  $^{18}\text{F}$ -SF51 warrants further evaluation in humans.

## Introduction

Brain inflammation upregulates 18 kDa translocator protein (TSPO), which is the most studied biomarker of neuroinflammation using positron emission tomography (PET) in neurologic [1] and psychiatric [2] disorders. The first PET radioligand for TSPO was  $^{11}\text{C}$ -PK11195 [3], which suffered from low specific signal and high nonspecific binding [4]. Although second-generation radioligands such as  $^{11}\text{C}$ -PBR28 [5] and  $^{11}\text{C}$ -DPA713 [6] had much higher specific binding than  $^{11}\text{C}$ -PK11195, all of these radioligands, including  $^{11}\text{C}$ -PK11195 [7], were sensitive to a co-dominantly expressed polymorphism of the three identified genotypes—high affinity binders (HABs), low affinity binders (LABs), and mixed affinity binders (MABs). LABs, which comprise 5–10% in the US and European populations, were found to have immeasurably low specific binding and thus needed to be excluded *a priori* from PET scans [4].

In the search for improved TSPO radioligands less sensitive to genotype, our laboratory developed the third-generation TSPO radioligand  $^{11}\text{C}$ -ER176 [8]. However,  $^{11}\text{C}$ -ER176 only partially overcame this problem. Although it has relatively lower sensitivity to genotype than  $^{11}\text{C}$ -PBR28, the sensitivity to genotype was high enough that it had to be corrected *a posteriori*. The unexpected advantage of  $^{11}\text{C}$ -ER176 was that it provided accurate values for LABs [9] due to a differential effect on the brain uptake of radiometabolites. As background, the accumulation of radiometabolites in brain can be indirectly measured as increasing values over time of the apparent receptor density (distribution volume ( $V_T$ )). Unlike  $^{11}\text{C}$ -PBR28 and  $^{11}\text{C}$ -DPA713,  $^{11}\text{C}$ -ER176 provided  $V_T$  values that were stable over increasing lengths of scanning [4]. Thus, while  $^{11}\text{C}$ -ER176 was sensitive to genotype, it was nevertheless an advance over the second-generation radioligands  $^{11}\text{C}$ -PBR28 and  $^{11}\text{C}$ -DPA713 because it provided accurate, time-stable  $V_T$  values in all three genotypes. Most notably, LABs did not need to be excluded prior to PET scanning using  $^{11}\text{C}$ -ER176; instead, the effect of genotype was corrected after the PET scan.

Building on this work, this study sought to develop an  $^{18}\text{F}$ -labeled analog of  $^{11}\text{C}$ -ER176 [10] because the longer half-life of  $^{18}\text{F}$  (109.8 min) compared to  $^{11}\text{C}$  (20.4 min) would allow it to be produced at a central radiopharmacy and distributed to distant imaging sites. Towards that end, six analogs of ER176 were synthesized that could be labeled with either  $^{11}\text{C}$  or  $^{18}\text{F}$ : three isomers with a fluoro group and three with a trifluoromethyl group at one of three positions (*ortho*, *meta*, and *para*) of the pendant aryl ring (Supplementary Fig. S1). Because radiolabeling these analogs was much easier using  $^{11}\text{C}$  than  $^{18}\text{F}$ , the performance of the six  $^{11}\text{C}$ -labeled analogs were compared in order to quantify TSPO in monkey brain [11]. The  $^{11}\text{C}$  labeled analog with  $^{19}\text{F}$ -fluorine in the *meta* position of the pendant aryl ring ( $^{11}\text{C}$ -SF12051, hereafter abbreviated to  $^{11}\text{C}$ -SF51) had a high ratio of specific to background uptake (whole brain  $BP_{\text{ND}} = 8.1$ ), excellent quantitation by compartmental modeling, and seemed suitable to extend to human participants.

However, while  $^{11}\text{C}$ -SF51 performed well in nonhuman primates [11], it was not clear that  $^{18}\text{F}$ -SF51 would do so because of possibly differential disposition of the radiolabeled metabolites.  $^{11}\text{C}$  and  $^{18}\text{F}$  labels are located at different positions of the molecule, and metabolism may generate different radiometabolites; some of these radiometabolites might accumulate in brain or its adjacent structures. For example,  $^{18}\text{F}$ -SF51 defluorination could generate  $^{18}\text{F}$  fluoride ions that could accumulate in the skull and that might thus contaminate quantitation of adjacent brain tissue. In contrast,  $^{11}\text{C}$ -SF51 defluorination would generate nonradioactive fluoride ions. Thus, before proceeding to a first-in-human study using  $^{18}\text{F}$ -SF51, it was necessary to ensure that this radioligand performs well in monkeys, which provide the best animal model for humans.

This study sought to determine whether  $^{18}\text{F}$ -SF51 provides accurate quantitation of TSPO in rhesus monkey brain. The density of the target ( $V_T$ ) was measured with compartmental modeling of the concentration of radioactivity in brain relative to the concentration of parent radioligand, separated from radiometabolites, in arterial plasma. Accuracy was assessed based on the known distribution of TSPO in

monkey brain, pharmacological blockade by the standard reference compound (PK11195), and goodness-of-fit of the compartmental modeling. In addition, because radiometabolite accumulation in brain has been a problem for some TSPO radioligands [9], we directly assessed whether radiometabolites were present in mouse brain extracts and indirectly assessed radiometabolite accumulation in monkey brain by the time stability of  $V_T$  with increasing scan duration.

## Material And Methods

### Radiochemistry

Synthesis of  $^{18}\text{F}$ -SF51 from a diaryliodonium salt [10] has previously been described. For this study,  $^{18}\text{F}$ -SF51 was prepared by a new method based on radiofluorination of a diarylselenone precursor according to a protocol recorded in FDA-sanctioned eIND #162310. Detailed information regarding synthesis of the precursor and radiosynthesis will be published separately.

### Animals

All studies were conducted in accordance with the ARRIVE guidelines for reporting animal research as well as the *Guidelines for the Care and Use of Laboratory Animals, 8th Edition* [12, 13]. All studies were approved by the National Institute of Mental Health Animal Care and Use Committee.

### PET Study in Rhesus Monkeys

Three male rhesus monkeys ( $10.0 \pm 1.8$  kg) were initially immobilized with ketamine hydrochloride (1 mg/kg, i.m.), anesthesia was maintained with 1.0–3.0% isoflurane and 98%  $\text{O}_2$ , and body temperature was maintained at between 37.0–37.5°C. Electrocardiogram, body temperature, heart rate, and respiratory rate measures were monitored throughout the scan.

Brain PET imaging was performed using a microPET Focus 220 camera (Siemens Medical Solution; Knoxville, TN). Following a transmission scan using a  $^{57}\text{Co}$  point source, 180-minute dynamic PET scans were acquired after IV injection of  $^{18}\text{F}$ -SF51 ( $198 \pm 32$  MBq, Supplementary Table S1). For baseline experiments, 20 mL of a vehicle containing 20% (2-hydroxypropyl)- $\beta$ -cyclodextrin and two equivalents of HCl were injected intravenously 10 minutes before radioligand administration. For the blocked experiment, PK11195 was dissolved in vehicle and then injected intravenously (5mg/kg) 10 minutes before radioligand injection for all three monkeys. One of the three monkeys underwent an additional blocked scan with 5 mg/kg of PBR28, performed using a MultiScan™ LFER 150 PET/CT (Mediso USA, LLC; Arlington, VA). The interval between baseline and blocked imaging sessions was at least three weeks in order to allow the monkey to recover from arterial blood sampling. Focus 220 PET images were histogrammed into 30 time frames (6×30, 3×60, 2×120, 4×300, and 15×600 seconds) and reconstructed using Fourier rebinning plus a two-dimensional filtered back-projection with scatter and attenuation correction. MultiScan LFER PET images were reconstructed with 3D-OSEM with two iterations and nine subsets and were corrected for scatter and attenuation.

# Parent Radioactivity and Radiometabolite Analysis in Plasma

Arterial blood sampling was performed in all scans to determine plasma parent concentration of the radioligand. Seventeen blood samples were drawn from an implanted port in the femoral artery of the monkeys during the 180-minute PET scans at 15-second intervals for the first two minutes, followed by samples at 3, 5, 10, 30, 60, 90, 120, 150, and 180 minutes (volumes varied from 1.0 to 5.0 mL).

Radioactivity in plasma was quantified and corrected for radiometabolites using high-performance liquid chromatography (HPLC). The separation was performed on an X-Terra  $C_{18}$  column (10  $\mu\text{m}$ , 7.8·300 mm) with an isocratic mobile phase composed of methanol: water: triethylamine (77.5:22.5:0.1 by vol.) at a flow rate of 5 mL/min. The plasma free fraction ( $f_p$ ) was measured by ultrafiltration, as previously described [14, 15]. A standard  $f_p$  was measured in a frozen aliquot of pooled plasma in parallel with the experimental blood sample, and as internal standard it was then used to normalize the measured  $f_p$  of the blood samples.

## Kinetic Analysis

PET images were co-registered to a standardized monkey MRI template using PMOD software (PMOD version 4.1, PMOD Technologies Ltd.; Zurich, Switzerland). Thirty-five predefined regions of interest (ROIs) from a monkey brain template were applied to the co-registered PET images to obtain regional time-activity curves. Brain uptake was expressed as standardized uptake value (SUV), which normalizes for injected radioactivity and body weight. Using the brain time-activity curves and the radiometabolite-corrected arterial input function, the total  $V_T$  was calculated with a two-tissue compartment model (2TCM). Lassen plot was used to determine target occupancy by PK11195 and nondisplaceable distribution volume ( $V_{ND}$ ), which was used to calculate binding potential ( $BP_{ND}$ ).

To determine the minimum scan duration needed to reliably measure  $V_T$  as well as to indirectly assess whether radiometabolites accumulate in the brain, the time stability of  $V_T$  was examined by truncating the scan duration from 180 minutes down to 30 minutes in 20-minute increments.

## PET Study in Mice

Imaging experiments were performed on a microPET Focus 120 camera (Siemens Medical Solution; Knoxville, TN). Mice were anesthetized with 1.5% isoflurane in oxygen at a flow rate of 1 L/min.  $^{18}\text{F}$ -SF51 (150  $\mu\text{L}$ ;  $2.9 \pm 0.6$  MBq) was injected intravenously through the tail vein of each mouse. Baseline scans were obtained in 12 mice, and another eight mice were imaged after pre-administration of 5 mg/kg PK11195. Scans were acquired for 120 minutes. Data were histogrammed into 24 time frames (6×20, 5×60, 4×120, 3×300, 3×600 and 3×1200 seconds) and reconstructed using Fourier rebinning plus a two-dimensional filtered back projection. No scatter or attenuation corrections were applied. PET images were analyzed using PMOD with a single ROI of the whole brain.

An *ex vivo* experiment was performed in another mouse 120 minutes after  $^{18}\text{F}$ -SF51 injection. Anticoagulated blood was withdrawn from the myocardium, and the brain was extracted. The harvested brain was weighed and immediately underwent radioanalysis. The plasma was separated by centrifugation, and the radioactivity in both whole blood and plasma was measured as previously described [14].

## Statistical Analysis

All statistical analyses were performed in GraphPad Prism (version 5.02 GraphPad Software, Inc, San Diego, California). Results with p-values < 0.05 were considered statistically significant. Data are presented as mean  $\pm$  standard deviation (SD) or mean with a range.

## Results

### Radiochemistry

Radiochemically stable  $^{18}\text{F}$ -SF51 was obtained for intravenous injection in sterile saline containing ethanol (10% v/v) in a total volume of 10 mL (Fig. 1). All preparations of  $^{18}\text{F}$ -SF51 had high radiochemical purity (> 99% by radio HPLC) and molar activity between 88.5 and 126 GBq/mmol (2.39–3.42 Ci/mmol).

### Arterial Input Function

The  $^{18}\text{F}$ -SF51 parent concentration peaked at  $4.1 \pm 0.4$  SUV with a steady washout that was well-fitted by a three-exponential function (Fig. 2A). The blocked plasma concentrations were higher than baseline both at the peak ( $7.5 \pm 1.7$  SUV) and during the rest of the curve (Fig. 2A), which was due to the displacement from blood cells and peripheral organs induced by PK11195 administration [7]. The mean  $f_p$  value of blocked scans ( $18.8 \pm 3.6\%$ ,  $n = 3$ ) was almost three-fold higher than that of baseline scans ( $6.4 \pm 0.7\%$ ,  $n = 3$ ).

With HPLC, the average percentage of parent in plasma 30 minutes post-injection was found to equal that of the radiometabolites (Supplementary Fig. S2A). At least five radiometabolites were more hydrophilic than the parent in plasma (Supplementary Fig. S2B).

### Brain Distribution and Kinetics in Monkeys

At baseline,  $^{18}\text{F}$ -SF51 readily entered monkey brain; its uptake peaked at five to 15 minutes post-injection (mean SUV peak  $2.0 \pm 0.1$ ) and was followed by moderate wash-out (Fig. 2B). Brain activity decreased to 50% of the peak by 110 minutes and to 30% of the peak by 180 minutes. The mean SUV peak after pre-blockade with 5 mg/kg PK11195 was higher ( $3.0 \pm 0.5$ ), and the wash-out phase was faster, likely because of reduced retention of the radioligand (Fig. 2B). As expected from the known distribution of TSPO in human and monkey brain [5], the activity was widespread and fairly uniform in the cortical gray

matter, cerebellum, and thalamus (Fig. 3). At baseline, a low uptake in the skull was observed (Supplementary Fig. S3) that did not affect brain quantification because it did not generate significant spill-over. This uptake was blocked by both PK11195 and PBR28 and is therefore likely due to extracerebral specific binding, not to deposition of  $^{18}\text{F}$ -fluoride ion into bone after defluorination.

## Quantification of $^{18}\text{F}$ -SF51 Binding in Monkey Brain

The brain time-activity curves were fitted well using a 2TCM for all the studied regions (Fig. 2B). The regions with the highest uptake were the amygdala, striatum, and insula ( $V_T/f_p$ : 242, 225, and 224  $\text{mL} \cdot \text{cm}^{-3}$ , respectively). Cerebellum had the lowest uptake (179  $\text{mL} \cdot \text{cm}^{-3}$ ). The coefficients of variation of  $V_T/f_p$ , calculated in 11 regions for each monkey, were within 30% (Table 1).  $V_T/f_p$  values were consistent among the three animals, with low inter-individual variability at baseline (10% variability).

Table 1  
Regional distribution volume corrected for plasma protein binding ( $V_T/f_p$ ) of  $^{18}\text{F}$ -SF51 in monkey brain (n = 3).

Region	$V_T/f_p$ ( $\text{mL} \cdot \text{cm}^{-3}$ )					
	Baseline			Blocked		
	Mean	SD	COV	Mean	SD	COV
Whole Brain	203	15	0.1	24	7	0.3
Frontal Cortex	201	11	0.1	26	8	0.3
Cingulate Cortex	218	16	0.1	25	7	0.3
Striatum	225	16	0.1	26	7	0.3
Insula	224	14	0.1	23	8	0.3
Temporal Cortex	209	21	0.1	22	7	0.3
Amygdala	242	22	0.1	23	5	0.2
Hippocampus	220	25	0.1	21	6	0.3
Thalamus	218	20	0.1	27	8	0.3
Parietal Cortex	202	10	0.0	24	7	0.3
Occipital Cortex	183	15	0.1	23	6	0.3
Cerebellum	179	21	0.1	26	8	0.3
COV: coefficient of variation; SD: standard deviation.						



A global measure of receptor occupancy by PK11195 was calculated using the Lassen plot, and the  $V_T/f_p$  was estimated by 2TCM. The occupancy was  $102 \pm 3\%$ .  $V_{ND}/f_p$ , determined as the x-intercept of the regression lines, was  $27 \pm 11 \text{ mL} \cdot \text{cm}^{-3}$  (Fig. 4).  $BP_{ND}$  was  $7.6 \pm 4.3$ , which was comparable to that of  $^{11}\text{C}$ -SF51 [11]. The results without  $f_p$  correction are shown in Supplemental Table S2.

Whole-brain  $V_T$  values were stable within 80 minutes of imaging. That is,  $V_T$  values were within 10% of that at 180 minutes, which suggests it requires at least 80 minutes to reliably measure  $V_T$ . It also suggests that radiometabolites were not accumulating in the brain (Fig. 5).

## Mouse Study

As previously described [10], PET images showed about 80% blockade of  $^{18}\text{F}$ -SF51 in mouse brain after i.v. administration of 5 mg/kg PK11195. Brain uptake at baseline reached peak values of  $\sim 0.8$  SUV at around 15 minutes and moderately washed out thereafter (Fig. 6A). After blockade with PK11195, brain uptake reached a peak of  $\sim 2.5$  SUV within three minutes and then washed out very rapidly. In the last 80 minutes of scanning, brain activity after blockade was 25% of that at baseline (Fig. 6B). The blockable high uptake ( $> 2$  SUV) was also found in lung, which is known to contain high levels of TSPO. No significant increase in radioactivity was detected in bone.

To determine whether radiometabolites entered the brain, one mouse was euthanized 120 minutes after injection of  $^{18}\text{F}$ -SF51, and the composition of the radioactivity in both the brain and plasma were measured with HPLC. Parent radioligand represented 96.4% of radioactivity in the brain but only 9.1% of radioactivity in plasma (Fig. 7), suggesting that radiometabolites generated in the plasma did not significantly enter the brain.

## Discussion

This study demonstrated that  $^{18}\text{F}$ -SF51 could accurately quantify TSPO density in rhesus monkey brain. The radioligand readily crossed the blood-brain barrier and had high uptake (peak SUV  $\sim 2$ ) followed by rapid wash-out from the brain. No significant defluorination was observed in the bones of the skull. Uptake in the skull was likely binding to TSPO on blood cells in the marrow, as this uptake was at least partially blocked by both PBR28 and PK11195. The uptake could not have been  $^{18}\text{F}$  fluoride in the bone, which could not have been blocked by TSPO ligands. In addition, distribution of SF51 in brain reflected the known distribution of TSPO and, in particular, reflected the pattern observed using  $^{11}\text{C}$ -SF51 in our previous primate studies [11]. Regions such as the amygdala, striatum, and cortex displayed high TSPO density, while cerebellum had the lowest binding. Furthermore, pre-blocking with PK11195 displaced about 90% of  $^{18}\text{F}$ -SF51 binding, which translated into a high  $BP_{ND}$  (7.6). This  $BP_{ND}$  value was similar to that observed for  $^{11}\text{C}$ -SF51 ( $BP_{ND} = 8.1$ ), which shares an identical chemical structure with  $^{18}\text{F}$ -SF51, as well as that of the structurally similar ER176 ( $BP_{ND} = 8.9$ ) [11]. The specificity of  $^{18}\text{F}$ -SF51 binding was

also corroborated by the mouse study, which showed a clear blockable effect not only in the brain, but also in the lungs, which are known to contain high levels of TSPO.

$V_T$  in the brain was well-identified using a 2TCM, and its value was relatively stable after 80 minutes of acquisition. This suggests that, despite position of the radiolabel in  $^{18}\text{F}$ -SF51 differing from that in  $^{11}\text{C}$ -SF51, no significant radiometabolite accumulated in the brain. In addition, the *ex vivo* mouse study showed that the radiometabolites found in plasma entered the brain at only negligible concentrations.

Plasma free fraction ( $f_p$ ) is directly related to the ability of the radioligand to cross the blood-brain barrier and bind to its target. Our measurements of  $f_p$  varied between baseline ( $6 \pm 1\%$ ) and blocked scans ( $19 \pm 4\%$ ), but we are confident that these measurements were accurate because of the consistency of  $f_p$  measurements drawn from an internal standard used in each study. Specifically,  $f_p$  was measured in a frozen aliquot of pooled plasma in parallel with the experimental blood samples, and the  $f_p$  values of this internal standard were then used to correct those of the blood samples. For the six PET scans reported in this paper (two per monkey), the  $f_p$  of the internal standard remained quite constant, ranging from 2.4 to 3.8%. The variation of  $f_p$  in the experimental samples was presumably not caused by variation of TSPO within white blood cells and platelets, as they compose a different compartment from the plasma. Radioligands, like other drugs, bind to numerous plasma proteins, and this binding rapidly equilibrates with the free concentration in plasma water. The variation of  $f_p$  measurements may thus have been caused by the displacement of blocker from plasma proteins; as an example, alpha-1-acid glycoprotein is one such component [16] for which drug-binding can be displaceable. This suggests that  $f_p$  can significantly increase in the presence of pharmacological dose of blocker [17].

Echoing the results of the present study, a new TSPO tracer,  $^{18}\text{F}$ -BIBD-239, was recently synthesized by introducing fluorine atoms into the aliphatic side chain of the ER176 terminal group [18]. *In vitro* competition binding assays showed that  $^{18}\text{F}$ -BIBD-239 has high affinity to TSPO, and animal models of stroke and glioma showed high and displaceable uptake in the lesions, although no significant displacement was observed in the healthy areas of the rat brain [18]. Although molecular docking calculations suggested that  $^{18}\text{F}$ -BIBD-239 might be insensitive to genotype, this can only be proven with human studies. It should be noted that ER176, whose structure is similar to that of  $^{18}\text{F}$ -BIBD-239, was initially thought to be insensitive to genotype on the basis of *in vitro* binding assays [8] but was subsequently discovered to be sensitive when injected into humans [9]. Similarly, the present study cannot determine whether SF51 is sensitive to genotype in humans, but we expect it to be. Indeed, in a competition binding assay against  $^3\text{H}$ -PK11195 using human brain homogenates, the LAB to HAB binding ratio was found to be 2.74, which is higher than that reported for ER176 (1.28) [8, 10]. If our future study in humans finds that  $^{18}\text{F}$ -SF51 is also sensitive to genotype, we nevertheless hope that—as with  $^{11}\text{C}$ -ER176—the specific binding of  $^{18}\text{F}$ -SF51 will be high enough to image LABs.

## Conclusion

This PET imaging study demonstrated that  $^{18}\text{F}$ -SF51 is an excellent radioligand with a good ratio of specific to nondisplaceable uptake as well as good time-stability of total TSPO receptor binding. Radiolabeling with  $^{18}\text{F}$  renders this ligand suitable for widespread use. Based on these findings,  $^{18}\text{F}$ -SF51 appears to be a promising next-generation TSPO PET ligand. Further evaluation in humans is warranted.

## Declarations

### *Funding*

This study was funded by the Intramural Research Program of the National Institute of Mental Health, National Institutes of Health (projects ZIA-MH002852 and ZIA-MH002793).

### *Competing Interests*

The authors have no conflict of interest to disclose, financial or otherwise.

### *Author Contributions*

XY: Acquired, analyzed, and interpreted the data; drafted and revised the manuscript; approved the final version of the manuscript.

FS: Acquired and analyzed the data; revised the manuscript; approved the final version of the manuscript.

J-SL: Acquired, analyzed, and interpreted the data; revised the manuscript; approved the final version of the manuscript.

CLM: Acquired and analyzed the data; revised the manuscript; approved the final version of the manuscript.

JAMS: Acquired and analyzed the data; revised the manuscript; approved the final version of the manuscript.

MJ: Acquired and analyzed the data; revised the manuscript; approved the final version of the manuscript.

LSM: Acquired and analyzed the data; revised the manuscript; approved the final version of the manuscript.

MVB: Acquired and analyzed the data; revised the manuscript; approved the final version of the manuscript.

SSZ: Acquired, analyzed, and interpreted the data; revised the manuscript; approved the final version of the manuscript.

VWP: Conceptualized and designed the study; acquired, analyzed, and interpreted the data; revised the manuscript for critical intellectual content; approved the final version of the manuscript.

RBI: Conceptualized and designed the study; acquired, analyzed, and interpreted the data; revised the manuscript for critical intellectual content; approved the final version of the manuscript.

PZ-F: Conceptualized and designed the study; acquired, analyzed, and interpreted the data; revised the manuscript for critical intellectual content; approved the final version of the manuscript.

### ***Data Availability***

The datasets generated during and/or analyzed during the current study are available from the corresponding author on reasonable request.

### ***Ethics Approval***

All studies were approved by the National Institute of Mental Health Animal Care and Use Committee.

### ***Consent to Participate***

Not applicable.

### ***Consent to Publish***

Not applicable.

## **References**

1. Kreisl WC, Kim MJ, Coughlin JM, Henter ID, Owen DR, Innis RB. PET imaging of neuroinflammation in neurological disorders. *Lancet Neurol.* 2020;19:940–50. doi:10.1016/s1474-4422(20)30346-x.
2. Shetty HU, Zoghbi SS, Morse CL, Kowalski A, Hirvonen J, Innis RB, et al. Development of a non-radiometric method for measuring the arterial input function of a (11)C-labeled PET radiotracer. *Sci Rep.* 2020;10:17350. doi:10.1038/s41598-020-73646-4.
3. Charbonneau P, Syrota A, Cruzel C, Valois JM, Prenant C, Cruzel M. Peripheral-type benzodiazepine receptors in the living heart characterized by positron emission tomography. *Circulation.* 1986;73:476–83. doi:10.1161/01.cir.73.3.476.
4. Fujita M, Kobayashi M, Ikawa M, Gunn RN, Rabiner EA, Owen DR, et al. Comparison of four (11)C-labeled PET ligands to quantify translocator protein 18 kDa (TSPO) in human brain: (R)-PK11195, PBR28, DPA-713, and ER176-based on recent publications that measured specific-to-non-displaceable ratios. *EJNMMI Res.* 2017;7:84. doi:10.1186/s13550-017-0334-8.
5. Briard E, Zoghbi SS, Imaizumi M, Gourley JP, Shetty HU, Hong J, et al. Synthesis and evaluation in monkey of two sensitive 11C-labeled aryloxyanilide ligands for imaging brain peripheral benzodiazepine receptors in vivo. *J Med Chem.* 2008;51:17–30. doi:10.1021/jm0707370.

6. James ML, Fulton RR, Henderson DJ, Eberl S, Meikle SR, Thomson S, et al. Synthesis and in vivo evaluation of a novel peripheral benzodiazepine receptor PET radioligand. *Bioorg Med Chem*. 2005;13:6188–94. doi:10.1016/j.bmc.2005.06.030.
7. Kreisl WC, Fujita M, Fujimura Y, Kimura N, Jenko KJ, Kannan P, et al. Comparison of [(11)C]-(R)-PK 11195 and [(11)C]PBR28, two radioligands for translocator protein (18 kDa) in human and monkey: Implications for positron emission tomographic imaging of this inflammation biomarker. *NeuroImage*. 2010;49:2924–32. doi:10.1016/j.neuroimage.2009.11.056.
8. Zanotti-Fregonara P, Zhang Y, Jenko KJ, Gladding RL, Zoghbi SS, Fujita M, et al. Synthesis and evaluation of translocator 18 kDa protein (TSPO) positron emission tomography (PET) radioligands with low binding sensitivity to human single nucleotide polymorphism rs6971. *ACS Chem Neurosci*. 2014;5:963–71. doi:10.1021/cn500138n.
9. Ikawa M, Lohith TG, Shrestha S, Telu S, Zoghbi SS, Castellano S, et al. 11C-ER176, a radioligand for 18-kDa translocator protein, has adequate sensitivity to robustly image all three affinity genotypes in human brain. *J Nucl Med*. 2017;58:320–5. doi:10.2967/jnumed.116.178996.
10. Siméon FG, Lee JH, Morse CL, Stukes I, Zoghbi SS, Manly LS, et al. Synthesis and screening in mice of fluorine-containing PET radioligands for TSPO: discovery of a promising (18)F-labeled ligand. *J Med Chem*. 2021;64:16731–45. doi:10.1021/acs.jmedchem.1c01562.
11. Lee JH, Simeon FG, Liow JS, Morse CL, Gladding RL, Montero Santamaria JA, et al. In vivo evaluation of six analogs of (11)C-ER176 as candidate (18)F-labeled radioligands for translocator protein 18 kDa (TSPO). *J Nucl Med*. 2022;63:1252–8. doi:10.2967/jnumed.121.263168.
12. National Research Council. *Guide for the Care and Use of Laboratory Animals*, 8th edition. Washington, DC: National Academies Press (US); 2011.
13. Percie du Sert N, Hurst V, Ahluwalia A, Alam S, Avey MT, Baker M, et al. The ARRIVE guidelines 2.0: Updated guidelines for reporting animal research. *PLoS Biol*. 2020;18:e3000410.
14. Zoghbi SS, Shetty HU, Ichise M, Fujita M, Imaizumi M, Liow JS, et al. PET imaging of the dopamine transporter with <sup>18</sup>F-FECNT: a polar radiometabolite confounds brain radioligand measurements. *J Nucl Med*. 2006;47:520–7.
15. Gandelman MS, Baldwin RM, Zoghbi SS, Zea-Ponce Y, Innis RB. Evaluation of ultrafiltration for the free-fraction determination of single photon emission computed tomography (SPECT) radiotracers: beta-CIT, IBF, and iomazenil. *J Pharm Sci*. 1994;83:1014–9. doi:10.1002/jps.2600830718.
16. Lockhart A, Davis B, Matthews JC, Rahmoune H, Hong G, Gee A, et al. The peripheral benzodiazepine receptor ligand PK11195 binds with high affinity to the acute phase reactant alpha1-acid glycoprotein: implications for the use of the ligand as a CNS inflammatory marker. *Nucl Med Biol*. 2003;30:199–206. doi:10.1016/s0969-8051(02)00410-9.
17. Huang Z, Ung T. Effect of alpha-1-acid glycoprotein binding on pharmacokinetics and pharmacodynamics. *Curr Drug Metab*. 2013;14:226–38.
18. Chen H, Jiang Z, Cheng X, Zheng W, Sun Y, Yu Z, et al. [(18)F]BIBD-239: (18)F-labeled ER176, a positron emission tomography tracer specific for the translocator protein. *Mol Pharm*.

## Figures

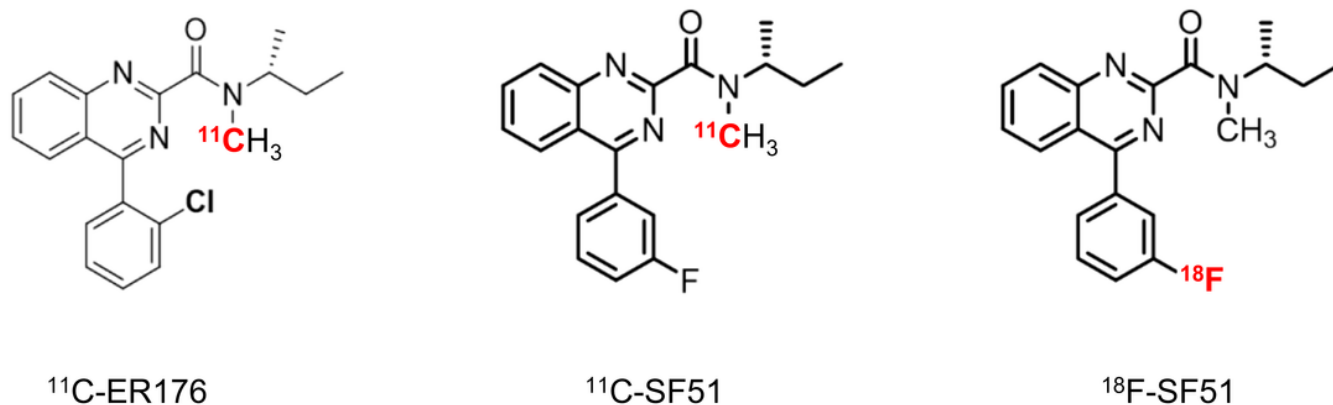


**Figure 1**

Chemical structures of  $^{11}\text{C}$ -ER176,  $^{11}\text{C}$ -SF51, and  $^{18}\text{F}$ -SF51.

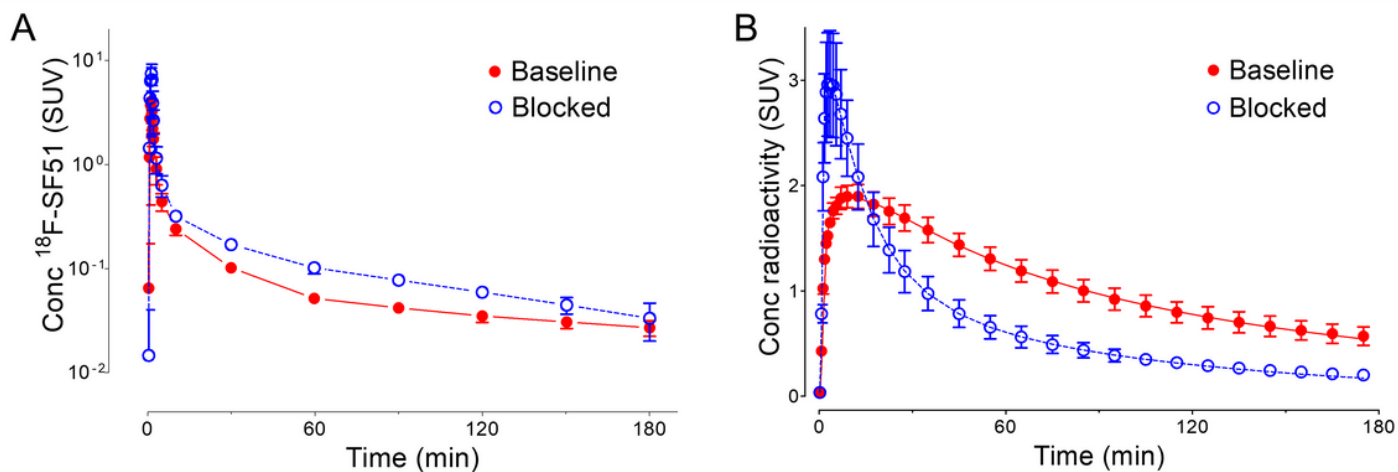


**Figure 2**

Concentration of  $^{18}\text{F}$ -SF51 in arterial plasma (**A**) and of radioactivity in whole brain (**B**) of rhesus macaques at baseline and after pre-blockade with PK11195. The selective 18kDa translocator protein (TSPO) ligand PK11195 (5 mg/kg i.v.) was injected 10 minutes prior to  $^{18}\text{F}$ -SF51. Concentration was expressed as standardized uptake value (SUV). Symbols and error bars represent mean and SD ( $n=3$ ), respectively.

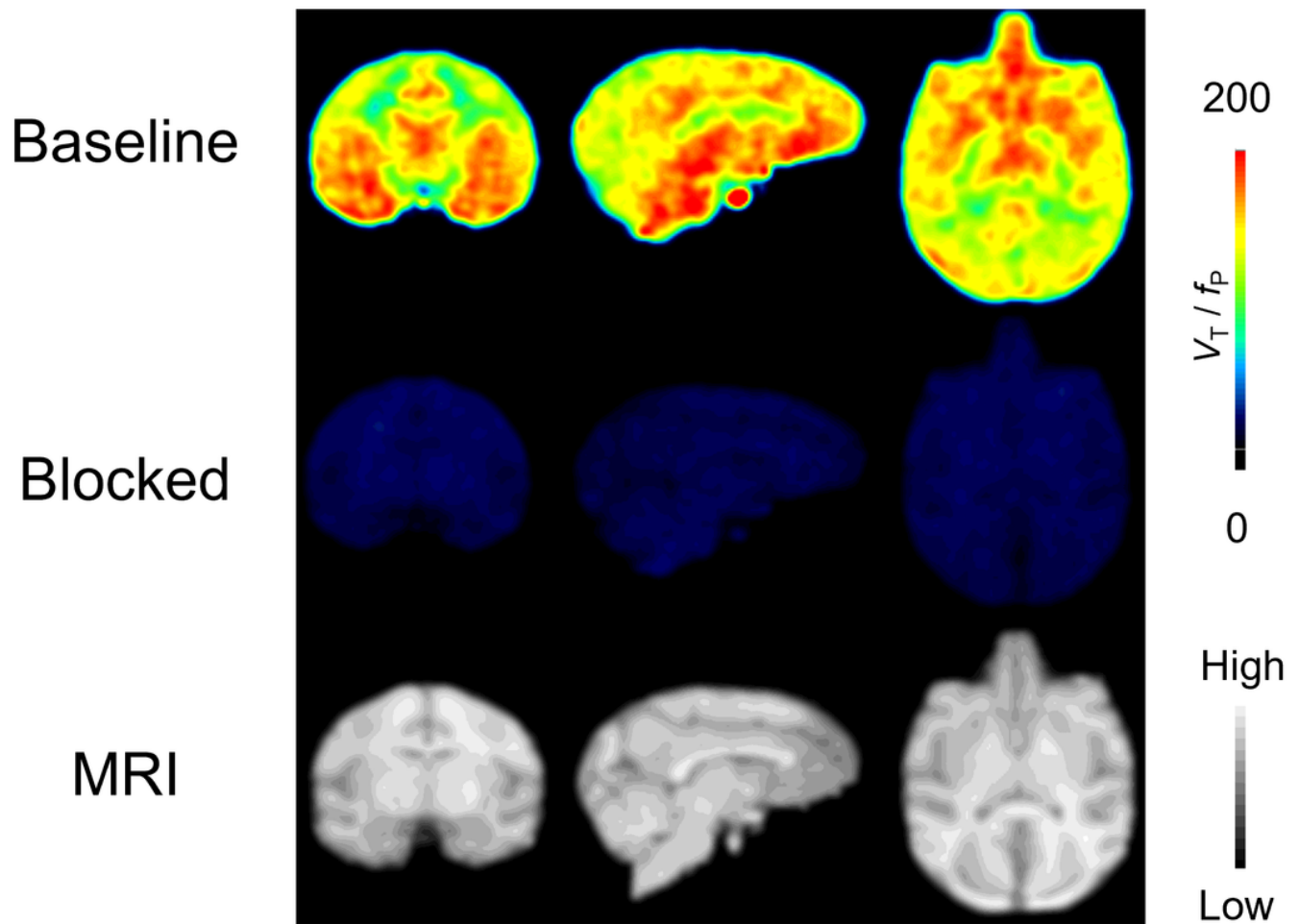


**Figure 3**

Parametric images of total 18kDa translocator protein (TSPO) binding ( $V_T/f_p$ ) for  $^{18}\text{F}$ -SF51 in monkey brain at baseline (top row) and after PK11195 pre-blockade (5 mg/kg, middle row). The individual monkey's MRI is shown in the bottom row. Each total distribution volume corrected for free parent fraction in plasma ( $V_T/f_p$ ) image was generated by Logan Plot using 0–180 minutes of PET data graphical analysis.

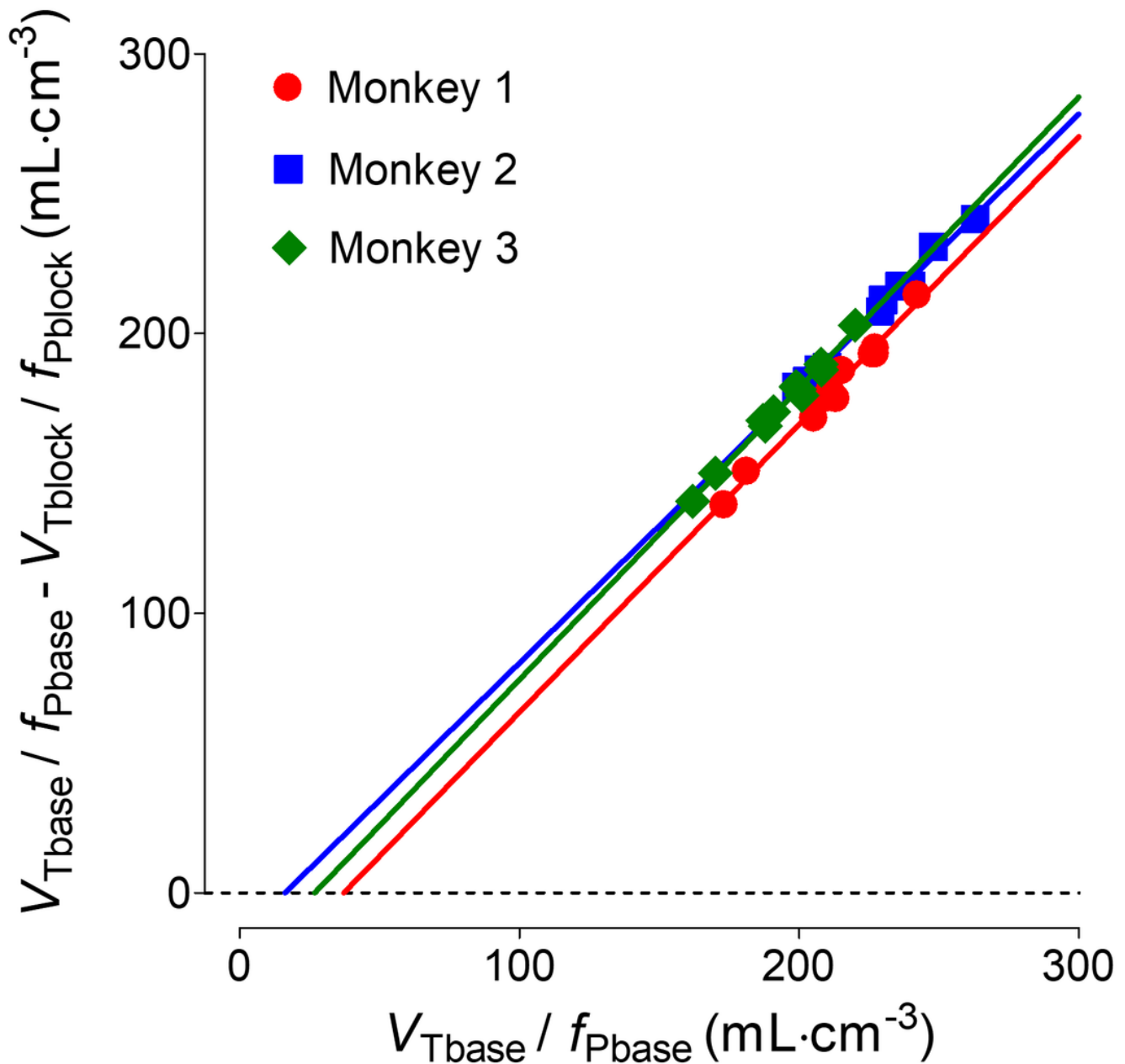


**Figure 4**

Receptor occupancy and nondisplaceable distribution volume ( $V_{ND}/f_p$ ) of <sup>18</sup>F-SF51 determined by Lassen plot. Data were from imaging studies in three rhesus monkeys at baseline and after administration of PK11195 at a dose of 5 mg/kg. The slope was  $1.02 \pm 0.03$  and the x-intercept was  $27 \pm 11$  (mean  $\pm$  SD, n=3). The R-squared values of linear fit were over 0.98.



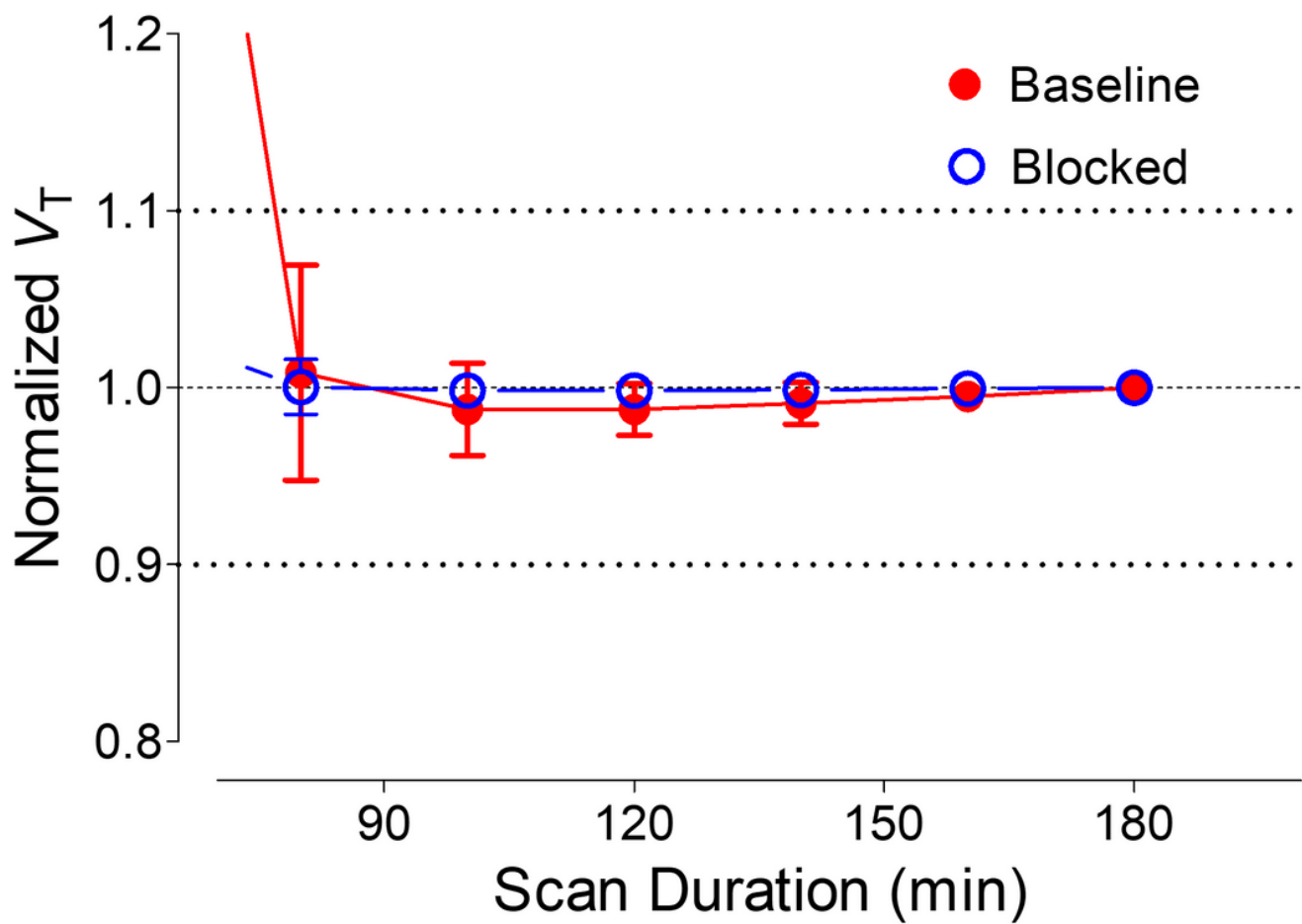
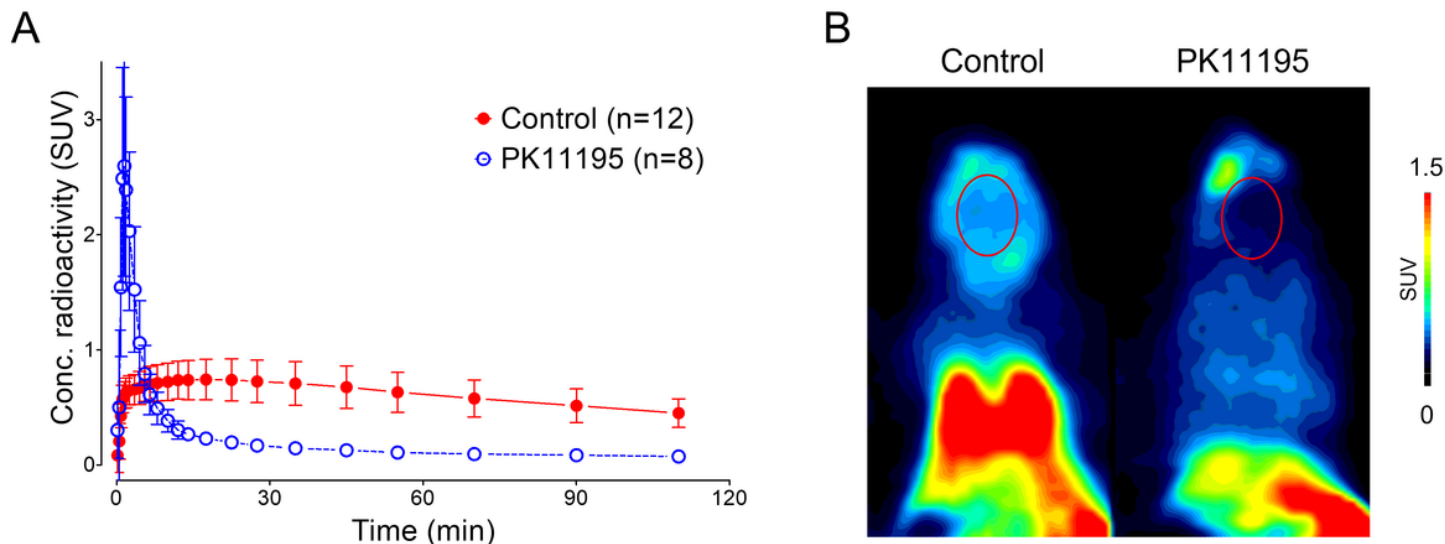


Figure 5

Time-stability analysis of whole-brain total distribution volume ( $V_T$ ) for  $^{18}\text{F}$ -SF51.  $V_T$  was calculated via two-tissue compartment modeling and normalized to the terminal  $V_T$  value at 180 minutes. Symbols and error bars represent the mean and SD (n=3).



**Figure 6**

Time-activity curves of whole-brain uptake **(A)** and representative standardized uptake value (SUV) images **(B)** in mice. PK11195 (5 mg/kg i.v.) was injected 10 minutes prior to  $^{18}\text{F}$ -SF51. SUV images were averaged over the last 40 minutes (60-100 minutes) of scan duration. The brain region is circled in red.

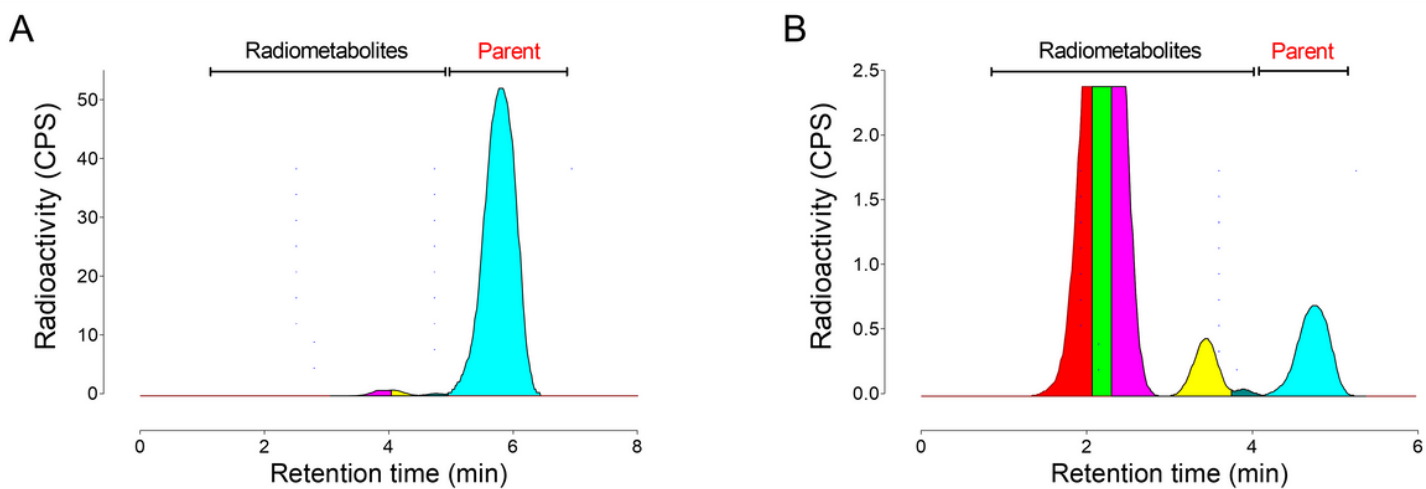


**Figure 7**

*Ex vivo* radio-chromatograms in mice 120 minutes after injection. Parent was 96.4% in brain **(A)** but only 9.1% in plasma **(B)**.

## Supplementary Files

This is a list of supplementary files associated with this preprint. Click to download.

- Yanetal18FSF51SUPPLEJNMMI101322.docx